DOI: 10.1002/ejic.200801186

Gold(I) Complexes of N-Heterocyclic Carbenes and Pyridines

Josh Y. Z. Chiou,[a] Shih C. Luo,[a] Wan C. You,[b] Amitabha Bhattacharyya,[a] C. Sekhar Vasam,[a] Cyong H. Huang,[a] and Ivan J. B. Lin*[a]

Keywords: Carbenes / Gold / Pyridine / Homogeneous catalysis / Luminescence / Oxidation

Overall ten ionic [Au(NHC)(Py)][PF_6]- and [Au_2(NHC)$_2$(Py)$_2$]-[PF_6]$_2$-type complexes [NHC = *N*,*N*′-dialkylbenzimidazol-2-ylidene, denoted as R_2-bimy with alkyl (R) being methyl (Me) or ethyl (Et), and Py = 4-substituted pyridine or 4,4′-bipyridine] have been prepared by incorporating various Pys into the Au^I-NHC core with Au(NHC)Cl as starting material. Their crystal structures characterized by X-ray diffraction indicate a linearly coordinated Au^I center and exhibit secondary forces such as Au···Au, Au···π, or π···π interactions. The luminescent properties of these compounds were studied in the solid state. Density-functional theory calculations on [Au(Me_2-bimy)(4-dmapy)][PF_6] [4-dmapy = 4-(dimethylamino)pyridine] predict the lowest electronic transition with nonzero oscillator strength is the fourth HOMO–LUMO transition. Whereas the fourth HOMO is mainly associated with the Py ligands, the LUMO is predominantly aurophilic. Four Au^I-NHC compounds were examined for their catalytic activity towards the oxidation of benzyl alcohol to aldehyde, in which the starting material [Au(Et_2-bimy)Cl] gave the highest yield.

Introduction

N-Heterocyclic carbenes (NHCs) are strong σ-donating and weak π-accepting ligands, which are relatively easy to generate and modify.[1,2] The electron-rich NHCs are versatile ligands in organometallic chemistry that often form strong bonds with metal atoms to produce stable complexes in different oxidation states. The unique properties of NHCs have led to the rising popularity of NHC-metal complexes.[2]

Au^I complexes possess many interesting properties, in particular, aurophilicity,[3,4] and luminescence.[5–7] Aurophilicity is a weak attractive force between closed-shell d^{10} Au^I centers with an energy comparable to that of a hydrogen bond. This attraction provides additional stability for molecular aggregation, both in the solid and in solution, and at times leads to luminescence.[5–8] Recently, research on the Au^I- and Au^{III}-catalyzed reactions has been booming,[9–11] earning the phrase "gold rush." It has been proposed that the catalytic property of gold may be affected by a relativistic contraction of 6s and expansion of 5d orbitals.[12]

Many [Au(NHC)X]-, [Au(NHC)$_2$][X]-, and [Au(NHC)-Y][X]-type compounds (where X = coordinated/noncoordinated anions and Y = neutral ligand) are known,[13,14] with their structural, catalytical, medicinal, liquid-crystal, and photophysical properties extensively studied.[15–20] Relatively less Au^I-Py (Py = pyridine derivatives) complexes have been studied, and only recently were their properties in luminescence,[6,7] catalysis,[6,21] and solution aggregation[6] reported.[6,7,21,22] Au^I complexes with both NHC and Py ligands could very likely give interesting results; however, very few such compounds have been examined.[23,24]

In this work, ten [Au(NHC)(Py)][PF_6]-type complexes are synthesized, in an attempt to gauge the influence of different 4-substituted pyridines on the structure, photophysical properties, and secondary attractive forces such as Au···Au, Au···π, and π···π interactions. In view of the increasing interest in Au^I-based catalysis, the preliminary results on the catalytic efficiency of a few Au^I-NHC complexes in benzyl alcohol oxidation are also reported.

Results and Discussion

Synthesis

Scheme 1 illustrates the synthetic pathway and lists the abbreviations for the ligands and compounds. The NHC ligands are *N*,*N*′-dialkylbenzimidazole-2-ylidene, denoted as R_2-bimy with alkyl (R) being methyl (Me) or ethyl (Et).

[a] Department of Chemistry, National Dong Hwa University, Hualien 97401, Taiwan
[b] Department of Chemistry, Fu Jen Catholic University, Taipei 24205, Taiwan
Supporting information for this article is available on the WWW under http://www.eurjic.org or from the author.

The Py ligands are 4-(dimethylamino)pyridine (4-dmapy), 4-picoline (4-pic), 4-phenylpyridine (4-phpy), 4-*tert*-butylpyridine (4-*t*bupy), 4-cyanopyridine (4-cyanopy), and 4,4′-bipyridine (4,4′-bpy). Table 1 gives the notations used to designate the ten [Au(NHC)(Py)] complexes. The starting materials [Au(NHC)Cl] were obtained by the Ag-carbene transfer route.[25] Direct addition of pyridines to the [Au(NHC)Cl] compounds in CH_2Cl_2 did not generate cationic $[Au(NHC)(Py)]^+$-type products. However, sequential treatment of [Au(NHC)Cl] with ethanolic $AgNO_3$, followed by 4-substituted pyridines and NH_4PF_6 would produce $[Au(NHC)(Py)][PF_6]$ complexes. Reaction of [Au(NHC)Cl] with $AgNO_3$ presumably formed an intermediate $[Au(NHC)(NO_3)]$ compound, as has been reported.[26]

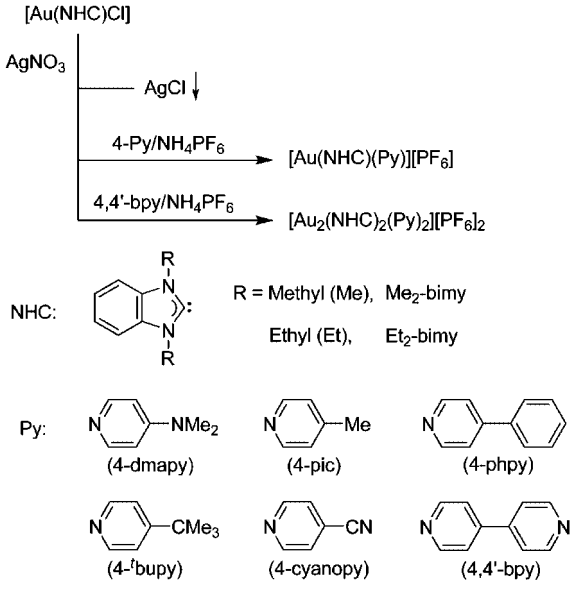

Scheme 1.

These $[Au(NHC)(Py)][PF_6]$ compounds are somewhat unstable in DMSO. The colorless solution changes from pink to purple overnight on dissolution at room temperature. At high temperature, the color changes immediately. This color change is a characteristic feature of Au-nanoparticle (Au-NP) formation. As a typical example, spherical Au-NPs produced from complex **6** with a uniform size of ca. 10 nm were observed by transmission electron microscopy (Figure 1). NHCs and pyridines are known to be efficient stabi-

Table 1. Notations for complexes.

Complex	Notation
$[Au(Me_2\text{-bimy})(4\text{-dmapy})][PF_6]$	**1**
$[Au(Et_2\text{-bimy})(4\text{-dmapy})][PF_6]$	**2**
$[Au(Me_2\text{-bimy})(4\text{-pic})][PF_6]$	**3**
$[Au(Et_2\text{-bimy})(4\text{-pic})][PF_6]$	**4**
$[Au(Me_2\text{-bimy})(4\text{-phpy})][PF_6]$	**5**
$[Au(Et_2\text{-bimy})(4\text{-phpy})][PF_6]$	**6**
$[Au(Et_2\text{-bimy})(4\text{-}t\text{bupy})][PF_6]$	**7**
$[Au(Et_2\text{-bimy})(4\text{-cyanopy})][PF_6]$	**8**
$[Au_2(Me_2\text{-bimy})_2(4,4'\text{-bpy})_2][PF_6]_2$	**9**
$[Au_2(Et_2\text{-bimy})_2(4,4'\text{-bpy})_2][PF_6]_2$	**10**

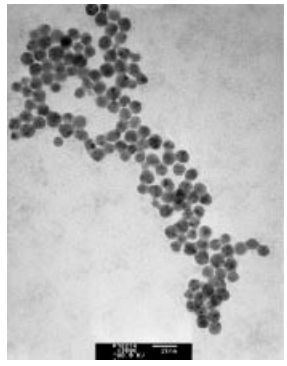

Figure 1. TEM image of Au-NPs.

Table 2. Selected chemical shifts in the ^{13}C NMR spectra [ppm], bond lengths [Å], and C–Au–N angles [°] for Au^I complexes.

Complex	δ(Au–C)[a]	Au–C	Au–N	C–Au–N
1	173.97	2.004(13)	2.041(11)	180.00(0)
2	172.45	2.003(9)	2.037(7)	179.173(334)
3	172.54	1.981(7)	2.064(6)	177.947(301)
4	171.03	1.975(4)	2.044(4)	179.320(174)
5	172.43	1.982(4)	2.054(4)	176.18(14)
6	170.80	1.983(4)	2.057(3)	177.591(145)
7	170.91	1.972(6)	2.061(5)	178.27(17)
8	170.94	1.977(5)	2.064(4)	177.53(16)
9	172.05	2.01(2)	2.050(18)	180.000(4)
10	170.56	1.979(5)	2.065(4)	178.92(17)
$[Au(Me_2\text{-bimy})Cl]$[b]	177.69[c]	1.985(11)	–	–
$[Au(Et_2\text{-bimy})Cl]$[b]	176.27[c]	2.01(3)	–	–
$[Au(Me_2\text{-bimy})_2][PF_6]$[d]	–	2.054(10)	–	–
$[Au(Et_2\text{-bimy})_2][PF_6]$[d]	–	2.024(12)	–	–
$[Au(4\text{-dmapy})_2][PF_6]$[e]	–	–	2.007(5)/2.012(5)	–
$[Au(4\text{-pic})_2][PF_6]$[e]	–	–	2.011(11)/2.016(11)	–
$[Au_2(L^1)_2][BF_4]_2$[f]	166.53	1.991(9)/2.000(8)	2.081(8)/2.087(8)	178.5(3)/179.4(3)
$[Au_2(L^2)_2][PF_6]_2$[g]	166.30[h]	2.00(5)/2.01(2)	2.040(17)/2.092(15)	174.3(8)/175.9(8)

[a] $[D_6]$DMSO. [b] Ref.[25a] [c] This work. [d] Ref.[25c] [e] Ref.[7] [f] L^1 = (Me)($PyCH_2$)-imy, ref.[23] [g] L^2 = [$PyCH_2$-imy-$(CH_2)_2$]$_2$O, ref.[24] [h] CD_3CN.

lizers for Au-NPs.[27,28] It is not surprising that Au-NPs formed from these compounds can be stabilized in solution without the addition of other stabilizers.

The ^{13}C NMR chemical shifts for the carbene carbon atom of these compounds range between δ = 170 and 174 ppm, whereas those of [Au(NHC)Cl] are found at $\delta \approx$ 177 ppm (Table 2). It is noted that the carbene carbon chemical shifts of the Me-substituted complexes are always downfield compared to those of the corresponding Et-substituted complexes by ca. 1.5 ppm. This could be attributed to the more electron-donating ability of the Et group than that of the Me group. These chemical shifts are not very sensitive to the Py substituents.

X-ray Crystallography

Structures of ten [Au(NHC)(Py)][PF_6] complexes were investigated by single-crystal X-ray diffraction. The details for the structure determination are given in the Supporting Information. Selected bonding parameters are given in the figure captions. ORTEP diagrams are presented with 50% probability ellipsoids; hydrogen atoms and $[PF_6]^-$ ions are omitted for clarity. All the molecular cations adopt a linear coordination. The Au–C and Au–N bond lengths are normal[6,13] as shown in Table 2. Most of the complexes can be described as an associated pair, shown as a dashed box in the figures. Secondary Au···Au (solid lines), π···π (dotted lines), and Au···π (dotted-dashed lines) interactions are often present. Apart from these interactions, the cations are further stabilized through CH···F hydrogen bonding with the $[PF_6]^-$ ions. Figures 2 to 11 depict the molecular structure and crystal packing of compounds **1**–**10**, respectively.

In Figure 2 of [Au(Me_2-bimy)(4-dmapy)][PF_6] (**1**) the short bond between the Py ring C and amine N [1.315(16) Å] is consistent with the delocalization of the amine lone pair with the Py ring, as observed previously.[13] The NHC and Py rings are coplanar, and the C–Au–N angle is perfectly linear. The molecular cations associate in an anti-parallel (head-to-tail) fashion to form a pair through weak Au···Au interactions [3.4728(1) Å] and NHC and Py ring π···π interactions [3.4159(0) Å]. A continuation of Au···Au and π···π interactions between pairs leads to a one-dimensional polymeric structure.

For [Au(Et_2-bimy)(4-dmapy)][PF_6] (**2**) in Figure 3 the two ethyl groups of an NHC ring point in opposite directions. Within the associated pair, an Au···Au distance of 3.5934(3) Å and π···π distance of 3.4356(52) Å are found. Between pairs, there are π···π [3.5421(46) Å] but no Au···Au interactions (>3.8 Å). The pairs stack in the form of col-

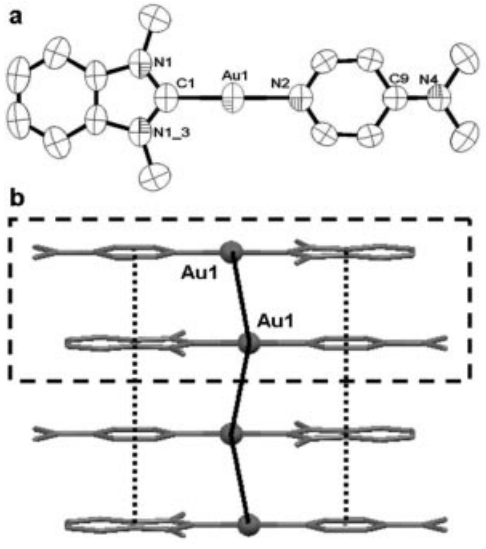

Figure 2. (a) ORTEP diagram of **1**. Selected bond lengths [Å], angles, and interplanar angles [°]: Au(1)–C(1) 2.004(13), Au(1)–N(3) 2.041(11), C(1)–N(1) 1.330(11), C(9)–N(4) 1.315(16); C(1)–Au(1)–N(3), 180.00, N(1)–C(1)–N(1′) 107.5(11). NHC–Py ring interplanar angle 0. (b) Packing diagram, at a small angle from the *a* axis.

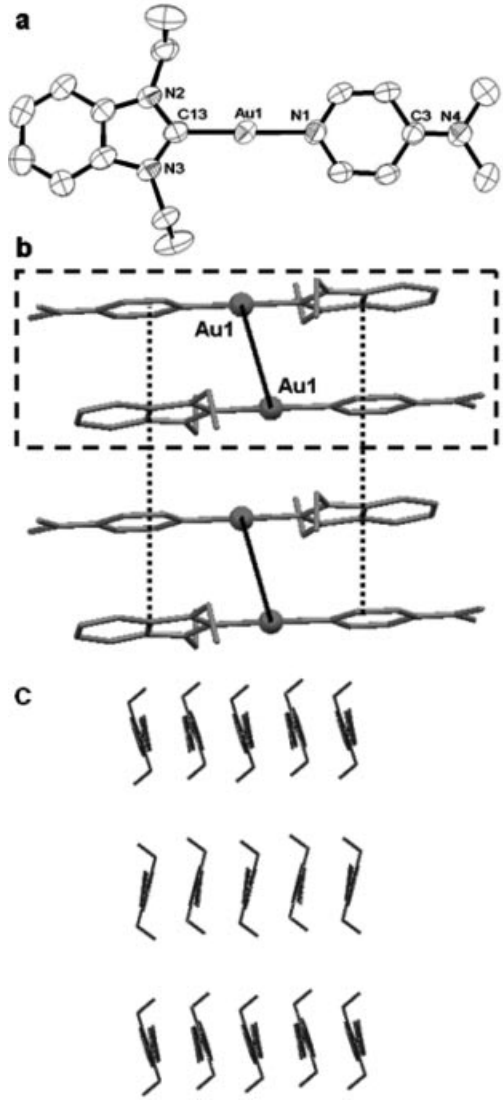

Figure 3. (a) ORTEP diagram of **2**. Selected bond lengths [Å], angles, and interplanar angles [°]: Au(1)–C(13) 2.003(9), Au(1)–N(1) 2.037(7), C(13)–N(2) 1.315(10), C(13)–N(3) 1.357(9), C(3)–N(4) 1.331(9); C(13)–Au(1)–N(1) 179.19(16), N(3)–C(13)–N(2) 108.4(7). NHC–Py ring interplanar angle 4.72. (b) Molecular packing, as seen along the *c* axis. (c) Herringbone packing, seen at a small angle to the *a* axis.

umns, which further arrange in a herringbone pattern, on seeing the molecules at a small angle to the *a* axis (Figure 3c).

For [Au(Me_2-bimy)(4-pic)][PF_6] (**3**) in Figure 4 the NHC and picolyl rings are almost coplanar, and the C–Au–N angle is 177.9°. In the dicationic pair, Au···Au [3.3517(3) Å] and ring π···π [3.4960(44) Å] interactions are observed. Between the pairs, there is a displacement so that the Au atoms of one pair are situated across the NHC ring of the neighboring pair with an Au···π distance of 3.5912(2) Å, close to the sum of the van der Waals radii of Au and C (3.50 Å). The presence of a similar weak η^2 interaction has been observed.[29]

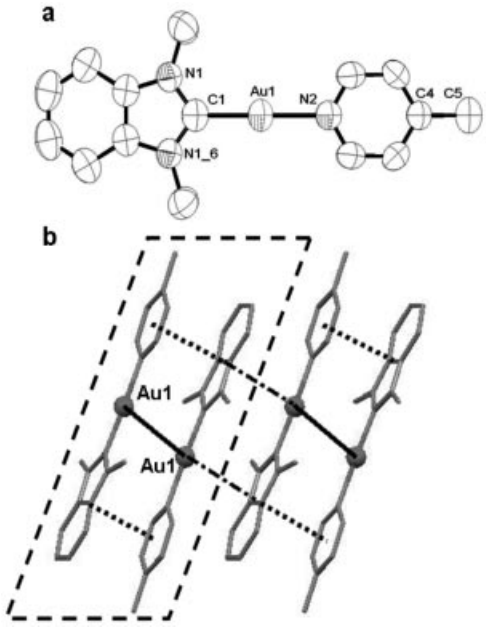

Figure 4. (a) ORTEP diagram of **3**. Selected bond lengths [Å], angles, and interplanar angles [°]: Au(1)–C(1) 1.981(7), Au(1)–N(2) 2.064(6), C(1)–N(1) 1.342(6), C(4)–C(5) 1.528(11); C(1)–Au(1)–N(3) 177.9(2), N(1)–C(1)–N(1′) 107.4(6). NHC–Py ring interplanar angle 1.17. (b) Packing diagram at a small angle from the *b* axis.

[Au(Et_2-bimy)(4-pic)][PF_6] (**4**) in Figure 5 has a C–Au–N angle of 179.31(15)°. The Et_2-bimy and 4-pic rings are essentially coplanar. In the pair, only Au···bimy ring interactions with a distance of 3.5128(2) Å are seen. The ethyl groups of each NHC ring point in the same direction, and away from the pair. There is no secondary interaction between the pairs, possibly due to the steric hindrances imposed by the ethyl side chain.

For [Au(Me_2-bimy)(4-phpy)][PF_6] (**5**) in Figure 6 the interplanar angle between the NHC and Py rings is 13.75°, whereas that of the Py and phenyl rings is 29.48°, giving a twisted appearance to the cation. The cation also deviates slightly from linearity, with a C–Au–N angle of 176.18(14)°. The cationic pair is associated through a weak Au···Au contact of 3.6040(5) Å.

In Figure 7 of [Au(Et_2-bimy)(4-phpy)][PF_6] (**6**) there is an interplanar angle of 13.85° between the NHC and Py rings, and of 16.78° between the Py and phenyl rings. The

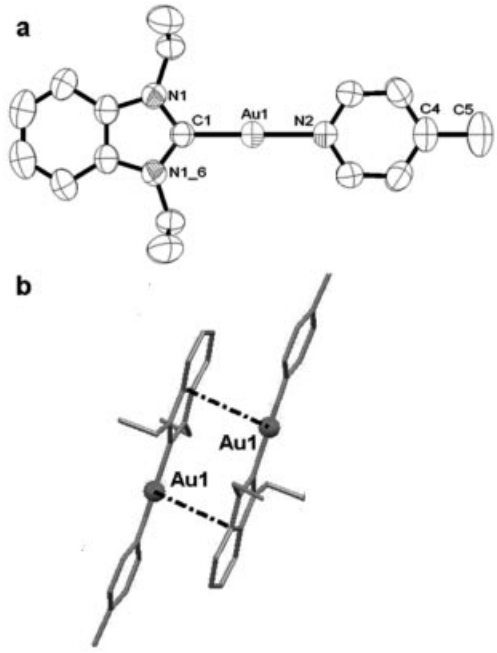

Figure 5. (a) ORTEP diagram of **4**. Selected bond lengths [Å], angles, and interplanar angles [°]: Au(1)–C(1) 1.975(4), Au(1)–N(2) 2.044(4), C(1)–N(1) 1.351(4), C(4)–C(5) 1.500(8); C(1)–Au(1)–N(2) 179.31(15), N(1)–C(1)–N(1′) 107.3(4). NHC–Py ring interplanar angle 0.60. (b) Crystal stacking, as seen at a small angle from the *b* axis.

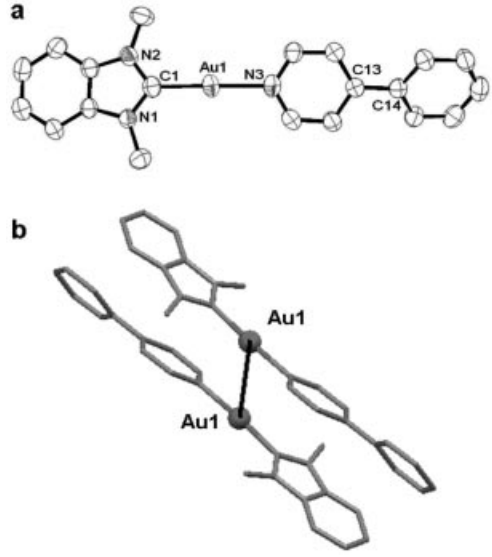

Figure 6. (a) ORTEP diagram of **5**. Selected bond lengths [Å], angles, and interplanar angles [°]: Au(1)–C(1) 1.982(4), Au(1)–N(3) 2.054(4), C(1)–N(1) 1.349(6), C(1)–N(2) 1.349(6), C(13)–C(14) 1.474(6); C(1)–Au(1)–N(3) 176.18(14), N(1)–C(1)–N(2) 107.2(4). NHC–Py ring interplanar angle 13.78, Py-phenyl ring interplanar angle 29.48. (b) Crystal stacking, seen along the *a* axis.

cations has a C–Au–N angle of 177.60(14)°. The two ethyl groups of an NHC ring point in opposite directions. The cations associate through a weak Au···Au contact of 3.5186(3) Å to form pairs. Between the pairs, there are ring

π···π interactions of 3.5065(36) Å, forming columns. The columns pack in a herringbone pattern, on seeing the cations along the *c* axis (Figure 7c).

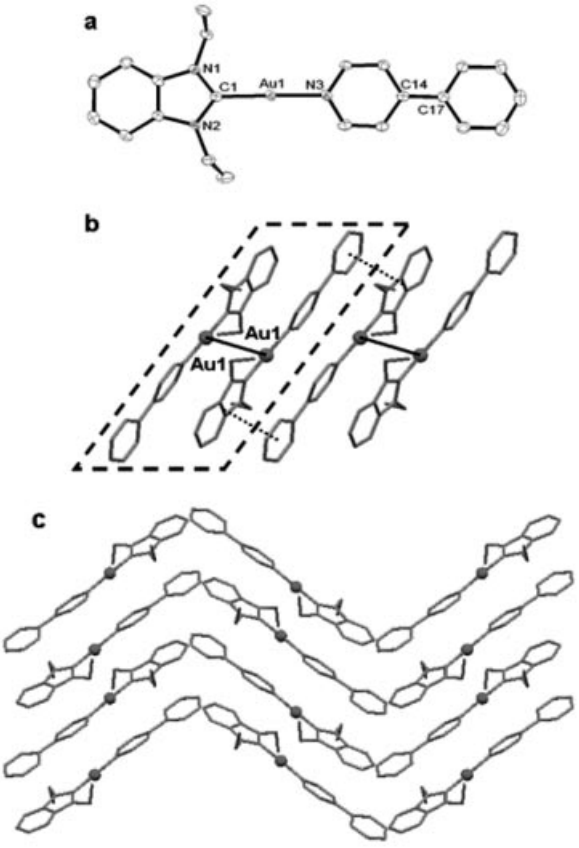

Figure 7. (a) ORTEP diagram of **6**. Selected bond lengths [Å], angles, and interplanar angles [°]: Au(1)–C(1) 1.983(4), Au(1)–N(3) 2.057(3), C(1)–N(1) 1.357(5), C(1)–N(2) 1.399(5), C(14)–C(17) 1.470(5); C(1)–Au(1)–N(3) 177.60(14), N(1)–C(1)–N(2) 109.2(3). NHC–Py ring interplanar angle 13.85, Py-phenyl ring interplanar angle 16.78. (b) Crystal stacking as seen along the *c* axis. (c) Herringbone pattern, seen along the *c* axis, rotated by 90° around normal to the plane of figure.

For [Au(Et_2-bimy)(4-*t*bupy)][PF_6] (**7**) in Figure 8 the NHC and Py rings are almost coplanar (interplanar angle 3.28°). The *tert*-butyl groups of the different cations are rotated, resulting in disorder. The cation is close to linear, with a C–Au–N angle of 178.27(17)°. Like in complex **4**, the Au atom of one cation is placed across the NHC ring of the other in a pair, with an Au···bimy ring contact of 3.5839(2) Å. The ethyl groups of each NHC ring point in the same direction, away from the pair. There is neither Au···Au nor Au···π interaction between the pairs.

In Figure 9 of [Au(Et_2-bimy)(4-cyanopy)][PF_6] (**8**) the NHC and Py rings are almost coplanar (interplanar angle 2.20°), and the C–Au–N angle is 177.53(16)°. The two ethyl groups at the NHC ring point in opposite directions. The Au^I atom does not participate in secondary interaction, rather, there are π···π interactions between pyridine rings [3.5996(40) Å] and between NHC and pyridine rings

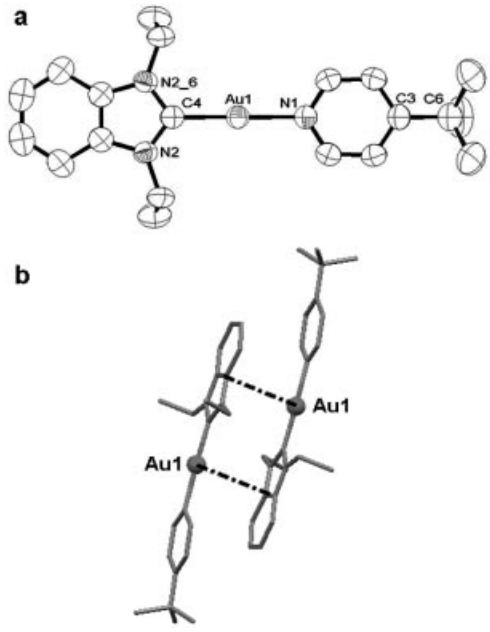

Figure 8. (a) ORTEP diagram of **7**. Selected bond lengths [Å], angles, and interplanar angles [°]: Au(1)–C(4) 1.972(6), Au(1)–N(1) 2.061(5), C(4)–N(2) 1.352(5); C(4)–Au(1)–N(1) 178.27(17), N(2)–C(12)–N(2′) 107.1(5). NHC–Py ring interplanar angle 3.28. (b) Crystal stacking at a small angle from the *b* axis.

[3.6411(43) Å]. In addition to the π···π interactions, the CN group interacts with an H atom of the Py ring of a neighboring cation at 2.6019(66) Å.

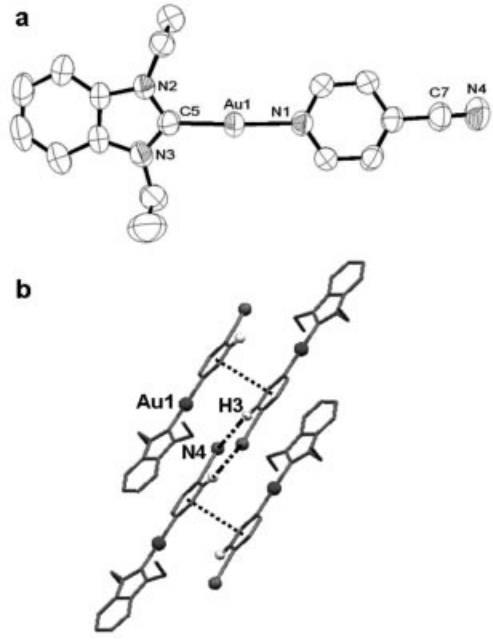

Figure 9. (a) ORTEP diagram of **8**. Selected bond lengths [Å], angles, and interplanar angles [°]: Au(1)–C(5) 1.977(5), Au(1)–N(1) 2.064(4), C(5)–N(3) 1.347(6), C(5)–N(2) 1.365(6), C(7)–N(4) 1.134(7); C(5)–Au(1)–N(1) 177.53(16), N(3)–C(5)–N(2) 107.5(4). NHC–Py ring interplanar angle 2.20. (b) Crystal stacking, along the *b* axis.

Figure 10 illustrates the bridging of two NHC-Au fragments through 4,4′-bipyridine to form $[Au_2(Me_2\text{-bimy})_2(4,4'\text{-bpy})_2][PF_6]_2$ (**9**). The geometry around the Au^I center is perfectly linear. The NHC and Py rings are coplanar, as are the two Py rings, giving a planar structure to the whole molecule. There is no aurophilic interaction in the packing of the cations. The two Au^I ions of a cation are sandwiched between the NHC rings of neighboring cations with Au···π and π···π interactions of 3.5222(0) Å. This extended arrangement and the interactions result in a two-dimensional array resembling a brick-laying pattern (Figure 10b).

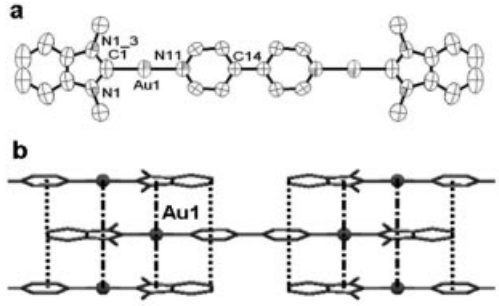

Figure 10. (a) ORTEP diagram of **9**. Selected bond lengths [Å], angles, and interplanar angles [°]: Au(1)–C(1) 2.01(2), Au(1)–N(1) 2.050(18), C(1)–N(1) 1.343(17), C(14)–C(14′) 1.52(4); C(1)–Au–N(11) 180.000(4), N(1)–C(1)–N(1′) 109(2). NHC–Py ring interplanar angle 0, Py–Py interplanar angle 0. (b) Crystal stacking along the *b* axis.

In Figure 11 of $[Au_2(Et_2\text{-bimy})_2(4,4'\text{-bpy})_2][PF_6]_2$ (**10**) the NHC and bpy moieties are not coplanar, but have an interplanar angle of 15.42°. The ethyl groups of each NHC ring point in the same direction, which is opposite to that of the ethyl groups of the other NHC. There are Au···bimy ring interactions of 3.5686(2) Å, seen only when the ethyl groups point away from each other.

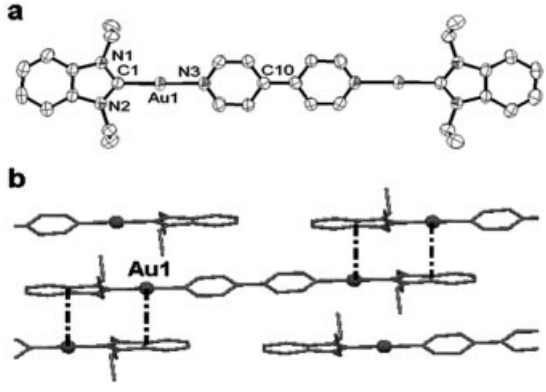

Figure 11. (a) ORTEP diagram of **10**. Selected bond lengths [Å], angles, and interplanar angles [°]: Au(1)–C(1) 1.979(5), Au(1)–N(3) 2.065(4), C(1)–N(1) 1.342(7), C(1)–N(2) 1.349(7); C(1)–Au(1)–N(3) 178.92(17), N(1)–C(1)–N(2) 107.2(4). NHC–Py ring interplanar angle 15.42, NHC–Py ring interplanar angle 1.97. (b) Packing diagram as seen along the *b* axis.

The involvement of Au^I in the secondary interactions of these compounds can be summarized as follows. Among the four *N*-methyl-substituted compounds, **1**, **3**, and **5** show Au···Au interactions, whereas **9** exhibits only extended Au···π interactions. Of the six *N*-ethyl-substituted compounds, **2** and **6** show Au···Au interactions, **4**, **7**, and **10** display Au···π interactions, and only **8** does not have the participation of Au^I in the secondary interactions. These results demonstrate the importance of the Au^I ion in the crystal packing.

The homoleptic compounds $[Au(NHC)_2][PF_6]$ and $[Au(Py)_2][PF_6]$ are taken as references for Au–NHC and Au–Py bond lengths, respectively, to compare with those of the $[Au(NHC)(Py)][PF_6]$-type compounds. Considering the set of compounds, **1**, $[Au(Me_2\text{-bimy})_2][PF_6]$, and $[Au(4\text{-dmapy})_2][PF_6]$, the Au–C bond length of 2.004(13) Å in **1** is 0.05 Å shorter than the 2.054(10) Å of $[Au(Me_2\text{-bimy})_2][PF_6]$, whereas the Au–N bond of 2.041(11) Å in **1** is ca. 0.031 Å longer than those of $[Au(4\text{-dmapy})_2][PF_6]$ [2.011(5)/2.016(5) Å].[7,25c] The trend persists on comparing compounds **3**, $[Au(Me_2\text{-bimy})_2][PF_6]$, and $[Au(4\text{-pic})_2][PF_6]$. In **3**, the Au–C bond is 0.073 Å shorter, whereas the Au–N bond is 0.049 Å longer. These differences in the bond length are larger than or equal to three times their standard deviations. The same trend of shorter Au–C and longer Au–N bonds is always observed for the other $[Au(NHC)(Py)]^+$-type compounds.

Photophysical Properties

As listed in Table 3, the UV/Vis spectra of these compounds exhibit two major absorption bands at ca. 230 and 290 nm, and a weaker band at ca. 250 nm in CH_3CN. Typical spectra for compounds **1** and **10** are given in Figure 12a and b. The starting compound $[Au(Et_2\text{-bimy})Cl]$[25a] possesses a structured band at ca. 270 nm, a small peak at 250 nm, and structureless bands at ca. 230 nm, whereas for $[Au(Py)_2][PF_6]$, a structureless band or shoulder is always observed at ca. 230 nm, and a low-energy band may occur between 250 and 290 nm.[6] The spectra of $[Au(NHC)(Py)][PF_6]$ appear to show the characteristics of both [Au(NHC)Cl] and $[Au(Py)_2][PF_6]$.

Table 3. Absorption and emission spectroscopic data for the complexes.

Complex	λ_{max} (ε_{max})/nm ($\times 10^4$ M^{-1} cm^{-1})	λ_{em}/nm	λ_{ex}/nm
1	229 (1.7), 255 (1.2), 286 (3.1)	402	366
2	229 (3.7), 256 (2.8), 287 (7.4)	389	346
3	226 (2.2), 287 (2.7)	470	356
4	225 (2.0), 287 (2.1)	397	296
5	223 (2.7), 253 (2.2), 287 (3.2)	453	326
6	223 (2.7), 251 (2.1), 287 (3.1)	447	348
7	225 (2.2), 253 (0.9), 287 (1.7)	460	361
8	227 (2.1), 254 (0.7), 287 (1.9)	411	360
9	226 (4.4), 245 (2.5), 286 (3.7)	453	348
10	226 (4.4), 247 (2.6), 287 (4.0)	448	336

All the complexes are luminescent in the solid state at room temperature upon excitation at ca. 350 nm. In Figure 12c, compound **1**, which has extended weak Au···Au interactions, displays a major structureless emission band at λ_{max} = 402 nm with a structured weak tail down to 600 nm

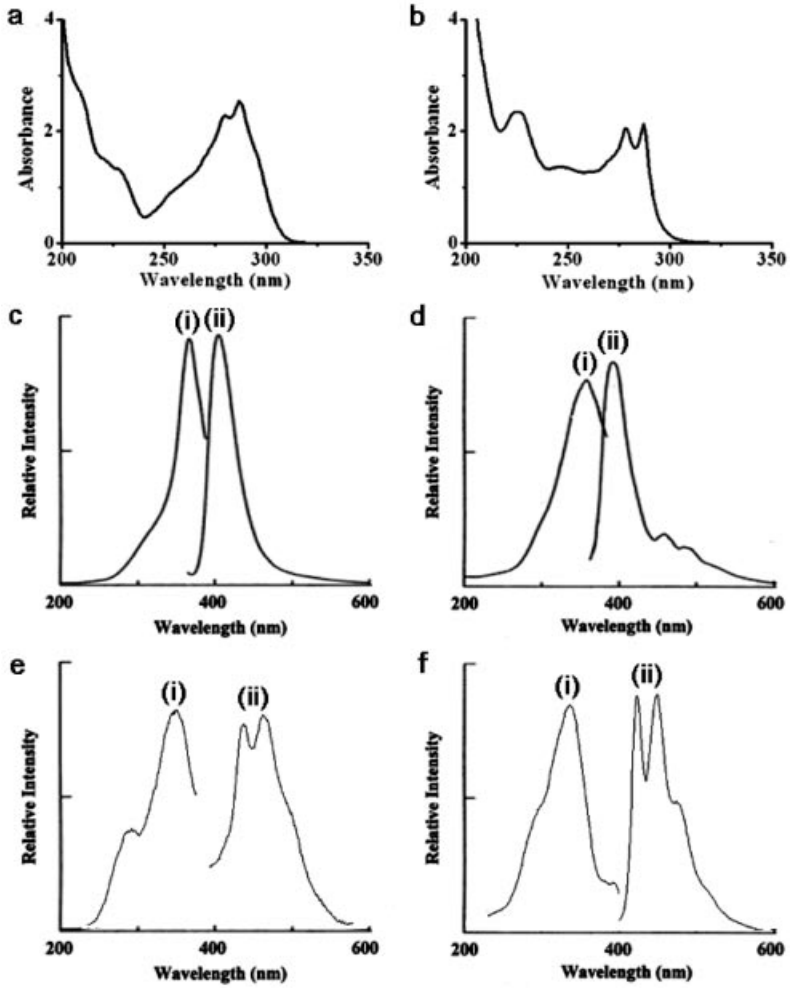

Figure 12. Electronic absorption spectra: (a) **1** and (b) **10**; emission spectra: (c) **1**, (d) **2**, (e) **9**, and (f) **10**. (i) Excitation, (ii) emission.

(excitation at λ_{max} = 366 nm). With an Au···Au interaction, compound **2** also displays a major sharp band at λ_{max} = 389 nm with an apparent structured tail. Density-functional[30] and time-dependent density-functional[31] B3LYP/LanLZDZ calculations were performed for complex **1** in the ground state and low-lying excited states, respectively. The dimeric $[Au(Me_2\text{-bimy})(4\text{-dmapy})]_2[PF_6]_2$ arranged as in the crystal structure was assumed in the calculation. The time-dependent density-functional calculations predict that the lowest electronic transition with nonzero oscillator strength is the fourth HOMO–LUMO transition. Figure 13 discloses that the fourth HOMO is associated mainly with the Py ligands, whereas the LUMO is predominantly of Au···Au interaction character. The calculations suggest that the electronic transitions involve both the ligands and Au^I ions. The structureless feature of the major emission band with structured tailing is consistent with theoretical calculations. Compounds **9** and **10**, both lacking Au···Au interactions, exhibit a structured emission at λ_{max} = 453 and 448 nm upon excitation at λ_{max} = 348 and 336 nm, respectively. The spacings in the fine structures are 1300–1500 cm^{-1}, in good agreement with the skeletal vibration frequencies of C=C and C=N bonds of the NHC and Py rings.[13,32] The emissive transitions of the latter two compounds are related mostly to the NHC and Py ligands. We

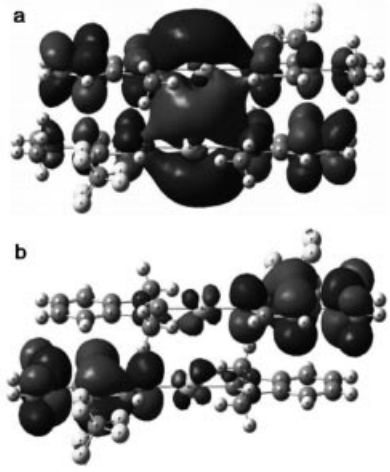

Figure 13. B3LYP/LanL2DZ molecular orbitals of $[Au(Me_2\text{-bimy})(4\text{-dmapy})]_2[PF_6]_2$. (a) LUMO and (b) the fourth HOMO.

did not observe a trend in the redshifting of absorption and emission bands with respect to the electron-accepting properties of Pys.[7]

Catalysis

The oxidation of benzyl alcohol to benzaldehyde catalyzed by Au^I complexes has been studied recently.[33] Excellent yields and selectivities were observed when AuCl with anionic β-diketiminate ligands were employed as catalysts. This reaction has been compared to the catalytic system of AuCl with PPh_3 or Py, in which a small amount of benzaldehyde was produced. The authors also made a simple comment that molecular sieves (4 Å) proved beneficial. We utilized [Au(NHC)(Py)][PF_6] and [Au(NHC)Cl] to carry out the catalytic oxidation of benzyl alcohol. Table 4 lists the preliminary results obtained under the general reaction conditions: 5 mol-% of Au^I-NHC compounds and an excess amount of *tert*-butyl hydroperoxide (TBHP) in toluene with molecular sieves (4 Å) at 90 °C for 24 h (Scheme 2). When complexes **2**, **6**, and **10** were used as catalysts, the respective yields of benzaldehyde were 60, 45, and 89% as in Entries 2, 3, and 4, compared to the reaction without a catalyst, which gave a yield of 13% (Entry 1). It has been suggested that coordination-saturated species should be avoided in catalytic reactions.[33] Our work, however, showed that [Au(NHC)(Py)][PF_6] compounds can be activated at 90 °C to provide fair yields of aldehyde; presumably the strong σ-donor ability of the NHCs could labilize the Pys. Under similar conditions, [Au(Et_2-bimy)Cl] (Entry 5) gave an essentially quantitative yield, comparable to that of Shi's group.[33] If the reaction was performed at room temperature, the yield dropped to 39% (Entry 6). We noticed that after the reaction, the powdery molecular sieves became pinkish, suggesting the impregnation of Au-NPs. Energy-dispersive X-ray spectroscopy (EDS) studies of the pinkish molecular sieves indeed showed the presence of Au, Al, S, and O. The pinkish color of the molecular sieves indicates that the catalytic system may involve colloidal AuNPs. Using poly(*N*-vinyl-2-pyrrolidone)-stabilized Au-NPs as a catalyst to oxidize benzyl alcohol in water under basic conditions has been reported, where benzoic acid was the sole product.[34]

Table 4. Catalytic oxidation of benzyl alcohol.

Entry	Catalyst	Yield [%][a]
1	no catalyst	13
2	complex **2**	60
3	complex **6**	45
4	complex **10**	89
5	[Au(Et_2-bimy)Cl]	99
6	[Au(Et_2-bimy)Cl]	39

[a] Estimated from GC analysis.

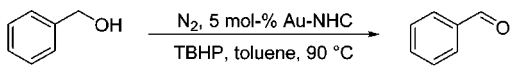

Scheme 2.

Conclusions

We describe the synthesis of ten [Au(NHC)(Py)][PF_6] compounds derived from [Au(NHC)Cl]. Crystal structures show that the Au^I ion plays an important role in the crystal packing through Au···Au or Au···π interactions. A general trend is observed that the Au–C bonds are longer whereas the Au–N bonds are shorter than in the corresponding homoleptic [Au(NHC)$_2$][PF_6] and [Au(Py)$_2$][PF_6] compounds, respectively.

Density-functional theory calculations based on dinuclear [Au(Me_2-bimy)(4-dmapy)]$_2$[PF_6]$_2$ indicates that the electronic transition involving the fourth HOMO is predominantly ligand in nature, whereas the LUMO has mainly Au···Au interaction character. In our earlier work, the HOMO and LUMO of [Au(4-dmapy)$_2$]$^{2+}$ are basically associated with ligands.[7] Thus, through a proper choice of ligands, it is possible to fine-tune the emission nature and perhaps create a molecular emitter.

Preliminary results on Au-NHC-catalyzed benzyl alcohol oxidation find that the [Au(NHC)(Py)][PF_6]-type compounds give fair yields, whereas [Au(Et_2-bimy)Cl] affords a much higher yield. Although Au-NPs may be involved in the catalytic process, further efforts are necessary to better understand the nature of this oxidation reaction.

Experimental Section

General Information: The NMR spectra were recorded with a Bruker Avance DPX_{300} spectrometer. Elemental analyses were performed by the Taiwan Instrumentation Center. UV/Vis spectra were recorded with a Hitachi U-3010 spectrophotometer. Fluorescence measurements were made by using an Amino BOWMAN series 2 spectrofluorometer. The TEM image was obtained with a JEOL JEM-301 microscopy instrument. Single-crystal X-ray data were collected with a Bruker SMART APEX II and a Siemens SMART CCD diffractometer. All the structures were solved and rened by employing SHELXL-97;[35] non-hydrogen atoms were rened anisotropically. Hydrogen atoms were placed in calculated positions. Compound **9** shows the presence of an unaccounted water molecule far from the NHC compound. The crystal data are given in the Supporting Information. CCDC-711510 (for **1**), -711511 (for **2**), -711512 (for **3**), -711513 (for **4**), -711514 (for **5**), -711515 (for **6**), -711517 (for **7**), -711519 (for **8**), -711520 (for **9**), -711521 (for **10**) contain the supplementary crystallographic data. These data can be obtained free of charge at www.ccdc.cam.ac.uk/data_request/cif or from Cambridge Crystallographic Data Centre, 12 Union Road, Cambridge CB2 1EZ.

Synthesis

[Au(Me_2-bimy)(4-dmapy)][PF_6] (1): $AgNO_3$ (22.1 mg, 0.13 mmol) in EtOH (5 mL) was added to [Au(Me_2-bimy)Cl] (49.4 mg, 0.13 mmol) in CH_2Cl_2 (10 mL). Immediate precipitation was observed. The resultant suspension was stirred for 10 min, and the precipitate was filtered. 4-dmapy (15.9 mg, 0.13 mmol) and NH_4PF_6 (21.2 mg, 0.13 mmol) were added to the filtrate, and the mixture was stirred at room temperature for 1 h. After the reaction, diethyl ether (30 mL) was added to precipitate the product. The precipitate was filtered and washed with EtOH to obtain the crude product. Recrystallization from CH_3CN/EtOH produced a colorless crystalline product. The yield was 67.4 mg, 85%. ^{1}H NMR

([D$_6$]DMSO): δ = 8.16 (d, ^3J = 6.3 Hz, 2 H, *o*-H of Py), 7.69–7.72 (m, 2 H, *o*-H of C_6H_4), 7.45–7.48 (m, 2 H, *m*-H of C_6H_4), 6.59 (d, ^3J = 6.3 Hz, 2 H, *m*-H of Py), 4.08 [s, 6 H, N(CH_3)], 2.93 [s, 6 H, N(CH_3)$_2$] ppm. ^{13}C NMR ([D$_6$]DMSO): δ = 173.97 (C-Au), 155.38, 150.34, 144.29, 133.93, 124.98, 112.52, 107.99, 107.40, 35.60, 35.41 ppm. $C_{16}H_{20}AuF_6N_4P$ (610.29): calcd. C 31.47, H 3.30, N 9.18; found C 30.97, H 3.63, N 9.12.

The following compounds were prepared according to a method similar to that of **1**. The molar quantities of the reagents used were about the same as those for **1**. Recrystallizations were carried out from the solvents mentioned.

[Au(Et$_2$-bimy)(4-dmapy)][PF$_6$] (2): Reagents: $AgNO_3$ (22.1 mg, 0.13 mmol), [Au(Et$_2$-bimy)Cl] (53.0 mg, 0.13 mmol), 4-dmapy (15.9 mg, 0.13 mmol), and NH_4PF_6 (21.2 mg, 0.13 mmol). Compound **2** was recrystallized from CH_2Cl_2/hexane. The yield was 71.4 mg, 86%. ^{1}H NMR ([D$_6$]DMSO): δ = 8.25 (d, ^3J = 6.4 Hz, 2 H, *o*-H of Py), 7.86–7.89 (m, 2 H, *o*-H of C_6H_4), 7.49–7.52 (m, 2 H, *m*-H of C_6H_4), 6.85 (d, ^3J = 6.4 Hz, 2 H, *m*-H of Py), 4.64 (q, ^3J = 6.9 Hz, 4 H, CH_2), 3.07 [s, 6 H, N(CH_3)$_2$], 1.47 (t, ^3J = 7.1 Hz, 6 H, CH_3) ppm. ^{13}C NMR ([D$_6$]DMSO): δ = 172.45 (C-Au), 155.41, 150.41, 132.88, 125.07, 112.69, 108.01, 44.08, 16.18 ppm. $C_{18}H_{24}AuF_6N_4P$ (638.34): calcd. C 33.87, H 3.79, N 8.78; found C 34.19, H 3.66, N 9.10.

[Au(Me$_2$-bimy)(4-pic)][PF$_6$] (3): Reagents: $AgNO_3$ (22.1 mg, 0.13 mmol), [Au(Me$_2$-bimy)Cl] (49.4 mg, 0.13 mmol), 4-pic (12.1 mg, 0.13 mmol), and NH_4PF_6 (21.2 mg, 0.13 mmol). Compound **3** was recrystallized from CH_2Cl_2/hexane. The yield was 56.7 mg, 75%. ^{1}H NMR ([D$_6$]DMSO): δ = 8.76 (d, ^3J = 5.0 Hz, 2 H, *o*-H of Py), 7.80–7.84 (m, 2 H, *o*-H of C_6H_4), 7.69 (s, 2 H, *m*-H of Py), 7.52–7.55 (m, 2 H, *m*-H of C_6H_4), 4.15 (s, 6 H, NCH_3), 2.60 (s, 3 H, CH_3) ppm. ^{13}C NMR ([D$_6$]DMSO): δ = 172.54 (C-Au), 151.45, 133.97, 127.80, 125.15, 112.66, 35.68, 21.47 ppm. $C_{15}H_{17}AuF_6N_3P$ (581.25): calcd. C 31.00, H 2.95, N 7.23; found C 31.04, H 2.90, N 7.59.

[Au(Et$_2$-bimy)(4-pic)][PF$_6$] (4): Reagents: $AgNO_3$ (22.1 mg, 0.13 mmol), [Au(Et$_2$-bimy)Cl] (53.0 mg, 0.13 mmol), 4-pic (12.1 mg, 0.13 mmol), and NH_4PF_6 (21.2 mg, 0.13 mmol). Compound **4** was recrystallized from CH_3CN/diethyl ether. The yield was 61.0 mg, 77%. ^{1}H NMR ([D$_6$]DMSO): δ = 8.76 (d, ^3J = 5.3 Hz, 2 H, *o*-H of Py), 7.89–7.94 (m, 2 H, *o*-H of C_6H_4), 7.70 (s, 2 H, *m*-H of Py), 7.51–7.56 (m, 2 H, *m*-H of C_6H_4), 4.67 (q, ^3J = 7.1 Hz, 4 H, CH_2), 1.45–1.57 (m, 9 H, CH_3) ppm. ^{13}C NMR ([D$_6$]DMSO): δ = 171.03 (C-Au), 154.44, 151.47, 132.89, 127.76, 125.21, 112.82, 112.70, 44.15, 21.46, 16.24 ppm. $C_{17}H_{21}AuF_6N_3P$ (609.30): calcd. C 33.51, H 3.47, N 6.90; found C 33.37, H 3.43, N 6.54.

[Au(Me$_2$-bimy)(4-phpy)][PF$_6$] (5): Reagents: $AgNO_3$ (22.1 mg, 0.13 mmol), [Au(Me$_2$-bimy)Cl] (49.4 mg, 0.13 mmol), 4-phpy (20.2 mg, 0.13 mmol), and NH_4PF_6 (21.2 mg, 0.13 mmol). Compound **5** was recrystallized from CH_3CN/EtOH. The yield was 65.2 mg, 78%. ^{1}H NMR ([D$_6$]DMSO): δ = 8.94 (s, 2 H, *o*-H of Py), 8.17 (s, 2 H, *m*-H of Py), 7.95 (d, ^3J = 3.8 Hz, 2 H, *o*-H of C_6H_5), 7.79–7.83 (m, 2 H, *o*-H of C_6H_4), 7.57–7.59 (m, 3 H, *m*-H of C_6H_5), 7.49–7.53 (m, 2 H, *m*-H of C_6H_4), 4.17 (s, 6 H, CH_3) ppm. ^{13}C NMR ([D$_6$]DMSO): δ = 172.43 (C-Au), 152.44, 133.95, 129.98, 127.93, 125.15, 124.00, 112.67, 35.70 ppm. $C_{20}H_{19}AuF_6N_3P$ (643.32): calcd. C 37.34, H 2.98, N 6.53; found C 37.28, H 3.00, N 6.49.

[Au(Et$_2$-bimy)(4-phpy)][PF$_6$] (6): Reagents: $AgNO_3$ (22.1 mg, 0.13 mmol), [Au(Et$_2$-bimy)Cl] (53.0 mg, 0.13 mmol), 4-phpy (20.2 mg, 0.13 mmol), and NH_4PF_6 (21.2 mg, 0.13 mmol). Compound **6** was recrystallized from CH_2Cl_2/hexane. The yield was 65.5 mg, 75%. ^{1}H NMR ([D$_6$]DMSO): δ = 8.93 (d, ^3J = 4.5 Hz, 2 H, *o*-H of Py), 8.20 (s, 2 H, *m*-H of Py), 7.98 (s, 2 H, *o*-H of C_6H_5), 7.89–7.92 (m, 2 H, *o*-H of C_6H_4), 7.59–7.61 (m, 3 H, *m*-H of C_6H_5), 7.51–7.54 (m, 2 H, *m*-H of C_6H_4), 4.70 (q, ^3J = 7.1 Hz, 4 H, CH_2); 1.50 (t, ^3J = 7.1 Hz, 6 H, CH_3) ppm. ^{13}C NMR ([D$_6$]DMSO): δ = 170.80 (C-Au), 152.22, 135.30, 132.79, 131.44, 130.04, 127.77, 125.29, 123.92, 112.62, 44.22, 16.11 ppm. $C_{22}H_{23}AuF_6N_3P$ (671.37): calcd. C 39.36, H 3.45, N 6.26; found C 39.35, H 3.48, N 6.26.

[Au(Et$_2$-bimy)(4-*t*bupy)][PF$_6$] (7): Reagents: $AgNO_3$ (22.1 mg, 0.13 mmol), [Au(Et$_2$-bimy)Cl] (53.0 mg, 0.13 mmol), 4-*t*bupy (17.6 mg, 0.13 mmol), and NH_4PF_6 (21.2 mg, 0.13 mmol). Compound **7** was recrystallized from CH_3CN/EtOH. The yield was 53.3 mg, 63%. ^{1}H NMR ([D$_6$]DMSO): δ = 8.79 (s, 2 H, *o*-H of Py), 7.89–7.92 (m, 4 H, *m*-H of Py and *o*-H of C_6H_4), 7.51–7.54 (m, 2 H, *m*-H of C_6H_4), 4.67 (q, ^3J = 7.1 Hz, 4 H, CH_2), 1.48 (t, ^3J = 7.1 Hz, 6 H, CH_3 of Et), 1.33 (s, 9 H, CH_3 of *t*bupy) ppm. ^{13}C NMR ([D$_6$]DMSO): δ = 170.91 (C-Au), 166.26, 151.50, 132.78, 125.29, 124.11, 112.59, 44.18, 38.70, 30.06, 16.06 ppm. $C_{20}H_{27}AuF_6N_3P$ (651.38): calcd. C 36.88, H 4.18, N 6.45; found C 36.98, H 3.96, N 6.54.

[Au(Et$_2$-bimy)(4-cyanopy)][PF$_6$] (8): Reagents: $AgNO_3$ (22.1 mg, 0.13 mmol), [Au(Et$_2$-bimy)Cl] (53.0 mg, 0.13 mmol), 4-cyanopy (13.5 mg, 0.13 mmol), and NH_4PF_6 (21.2 mg, 0.13 mmol). Compound **8** was recrystallized from CH_3CN/EtOH. The yield was 49.2 mg, 61%. ^{1}H NMR ([D$_6$]DMSO): δ = 9.12 (s, 2 H, *o*-H of Py), 8.25 (s, 2 H, *m*-H of Py), 7.81–7.85 (m, 2 H, *o*-H of C_6H_4), 7.52–7.55 (m, 2 H, *m*-H of C_6H_4), 4.63 (s, 4 H, CH_2); 1.48 (t, ^3J = 7.1 Hz, 6 H, CH_3) ppm. ^{13}C NMR ([D$_6$]DMSO): δ = 189.66 (CN), 169.56 (C-Au), 152.91, 133.00, 132.88, 128.80, 125.29, 116.40, 112.87, 112.70, 44.18, 16.22 ppm. $C_{15}H_{14}AuF_6N_4P$ (592.23): calcd. C 30.42, H 2.38, N 9.46; found C 30.30, H 2.41, N 9.50.

[{Au(Me$_2$-bimy)}$_2$(4,4′-bpy)$_2$][PF$_6$]$_2$ (9): Reagents: $AgNO_3$ (44.2 mg, 0.26 mmol), [Au(Me$_2$-bimy)Cl] (98.7 mg, 0.26 mmol), 4,4′-bpy (20.2 mg, 0.13 mmol), and NH_4PF_6 (42.4 mg, 0.26 mmol). Compound **9** was recrystallized from DMF/diethyl ether. The yield was 91.4 mg, 62%. ^{1}H NMR ([D$_6$]DMSO): δ = 9.13 (s, 4 H, *o*-H of Py), 8.41 (s, 4 H, *m*-H of Py), 7.83–7.86 (m, 4 H, *o*-H of C_6H_4), 7.54–7.58 (m, 4 H, *m*-H of C_6H_4), 4.18 (s, 12 H, CH_3) ppm. ^{13}C NMR ([D$_6$]DMSO): δ = 172.05 (C-Au), 152.94, 134.09, 133.98, 125.21, 124.89, 112.69, 35.73, 35.41 ppm. $C_{28}H_{28}Au_2F_{12}N_6P_2$ (1132.43): calcd. C 29.70, H 2.49, N 7.42; found C 29.32, H 2.66, N 7.38.

[{Au(Et$_2$-bimy)}$_2$(4,4′-bpy)$_2$][PF$_6$]$_2$ (10): Reagents: $AgNO_3$ (44.2 mg, 0.26 mmol), [Au(Et$_2$-bimy)Cl] (106.0 mg, 0.26 mmol), 4,4′-bpy (20.2 mg, 0.13 mmol), and NH_4PF_6 (42.4 mg, 0.26 mmol). Compound **10** was recrystallized from DMF/diethyl ether. The yield was 100.6 mg, 65%. ^{1}H NMR ([D$_6$]DMSO): δ = 9.11 (s, 4 H, *o*-H of Py), 8.38 (s, 4 H, *m*-H of Py), 7.91–7.94 (m, 4 H, *o*-H of C_6H_4), 7.53–7.56 (m, 4 H, *m*-H of C_6H_4), 4.70 (q, ^3J = 7.0 Hz, 4 H, CH_2), 1.51 (t, ^3J = 7.0 Hz, 6 H, CH_3) ppm. ^{13}C NMR ([D$_6$]DMSO): δ = 170.56 (C-Au), 152.99, 132.92, 125.27, 125.09, 112.88, 112.71, 44.20, 16.27 ppm. $C_{32}H_{36}Au_2F_{12}N_6P_2$ (1188.53): calcd. C 32.34, H 3.05, N 7.07; found C 32.62, H 3.37, N 7.04.

Oxidation of Alcohols with Au^I-NHC Compounds: [Au(Et$_2$-bimy)-Cl] (20.3 mg, 0.05 mmol) in toluene (0.50 mL) and seven beads of molecular sieves (4 Å) were placed in a flask under nitrogen. Benzyl alcohol (1 mmol) was added quickly followed by a TBHP (2 mL) solution (1.0 mol/L in toluene). The mixture was heated to 90 °C, stirred for 24 h, and monitored by GC. Product yields were determined by GC, with decane as internal standard. Similar reaction conditions were employed for all the oxidation experiments.

Theoretical Calculations: The calculations were carried out by using density-functional and time-dependent density-functional B3LYP with LanL2DZ basis sets.[30,31] With basis set LanL2DZ, the ab initio effective core potentials were employed to replace the core electrons of Au, in which mass-velocity and Darwin relativistic effects have been incorporated. The Gaussian 03 program[36] was utilized in the ab initio electronic structure calculations.

Supporting Information (see footnote on the first page of this article): Crystallographic data and refinement parameters.

Acknowledgments

We acknowledge the financial support from the National Science Council (Taiwan, ROC) (NSC 97-2113-M-259-009-MY3) and the National Center for High-Performance Computing of Taiwan for computer resources. A. B. thanks St. Joseph's College, Darjeeling 734104, West Bengal, India for granting leave to work in NDHU.

[1] F. Glorius, *Top. Organomet. Chem.* **2007**, *21*, 1–20.
[2] S. P. Nolan, *N-Heterocyclic Carbenes in Synthesis*, 1st ed., Wiley-VCH, Weinheim, **2006**.
[3] a) H. Schmidbaur, A. Schier, *Chem. Soc. Rev.* **2008**, *37*, 1931–1951; b) H. Schmidbaur, *Gold Bull.* **2000**, *33*, 3–10.
[4] a) P. Pyykko, *Chem. Soc. Rev.* **2008**, *37*, 1967–1997; b) P. Pyykko, *Angew. Chem. Int. Ed.* **2004**, *43*, 4412–4456.
[5] a) V. W. W. Yam, E. C. C. Cheng, *Chem. Soc. Rev.* **2008**, *37*, 1806–1813; b) R. L. White-Morris, M. M. Olmstead, A. L. Balch, *J. Am. Chem. Soc.* **2003**, *125*, 1033–1040; c) M. A. Rawashdeh-Omary, M. A. Omary, H. H. Patterson, J. P. Fackler, *J. Am. Chem. Soc.* **2001**, *123*, 11237–11247.
[6] J. C. Y. Lin, S. S. Tang, C. S. Vasam, W. C. You, T. W. Ho, C. H. Huang, B. J. Sun, C. Y. Huang, C. S. Lee, W. S. Hwang, A. H. H. Chang, I. J. B. Lin, *Inorg. Chem.* **2008**, *47*, 2543–2551.
[7] E. J. Fernández, A. Laguna, J. M. L. Luzuriaga1, M. Monge1, M. Montiel, M. E. Olmos, J. Pérez, M. Rodríguez-Castillo, *Gold Bull.* **2007**, *40*, 172–183.
[8] S. S. Tang, C. P. Chang, I. J. B. Lin, L. S. Liou, J. C. Wang, *Inorg. Chem.* **1997**, *36*, 2294–2300.
[9] S. P. Nolan, *Nature* **2007**, *445*, 496–497.
[10] N. Marion, S. P. Nolan, *Chem. Soc. Rev.* **2008**, *37*, 1776–1782.
[11] C. D. Pina, E. Falletta, L. Prati, M. Rossi, *Chem. Soc. Rev.* **2008**, *37*, 2077–2095.
[12] D. J. Gorin, F. D. Toste, *Nature* **2007**, *446*, 395–403.
[13] I. J. B. Lin, C. S. Vasam, *Can. J. Chem.* **2005**, *83*, 812–825.
[14] H. G. Raubenheimer, S. Cronje, *Chem. Soc. Rev.* **2008**, *37*, 1998–2011.
[15] S. K. Schneider, W. A. Herrmann, E. Herdtweck, *Z. Anorg. Allg. Chem.* **2003**, *629*, 2363–2370.
[16] a) B. L. Ricard, F. Gagosz, *Organometallics* **2007**, *26*, 4704–4707; b) D. V. Partyka, A. J. Esswein, M. Zeller, A. D. Hunter, T. G. Gray, *Organometallics* **2007**, *26*, 3279–3282; c) D. S. Laiter, P. Müller, T. G. Gray, J. P. Sadighi, *Organometallics* **2005**, *24*, 4503–4505.
[17] P. J. Barnard, S. J. Berners-Price, *Coord. Chem. Rev.* **2007**, *251*, 1889–1902.
[18] A. S. K. Hashmi, *Chem. Rev.* **2007**, *107*, 3180–3211.
[19] D. Krishnamurthy, M. R. Karver, E. Fiorillo, V. Orru, S. M. Stanford, N. Bottini, M. Barrios, *J. Med. Chem.* **2008**, *51*, 4790–4795.
[20] K. M. Lee, C. K. Lee, I. J. B. Lin, *Angew. Chem. Int. Ed. Engl.* **1997**, *36*, 1850–1852.
[21] Z. Li, X. Ding, C. He, *J. Org. Chem.* **2006**, *71*, 5876–5880.
[22] M. Freytag, P. G. Jones, *Chem. Commun.* **2000**, 277–278.
[23] V. M. Catalano, A. L. Moore, *Inorg. Chem.* **2005**, *44*, 6558–6566.
[24] B. Liu, W. Chen, S. Jin, *Organometallics* **2007**, *26*, 3660–3667.
[25] a) H. M. J. Wang, C. Y. L. Chen, I. J. B. Lin, *Organometallics* **1999**, *18*, 1216–1223; b) I. J. B. Lin, C. S. Vasam, *Comments Inorg. Chem.* **2004**, *25*, 75–129; c) H. M. J. Wang, C. S. Vasam, T. Y. R. Tsai, S. Chen, A. H. H. Chang, I. J. B. Lin, *Organometallics* **2005**, *24*, 486–493; d) I. J. B. Lin, C. S. Vasam, *Coord. Chem. Rev.* **2007**, *251*, 642–670.
[26] M. V. Baker, P. J. Barnard, S. K. Brayshaw, J. L. Hickey, B. W. Skelton, A. H. White, *Dalton Trans.* **2005**, 37–43.
[27] L. Zhao, C. Zhang, L. Zhuo, Y. Zhang, J. Y. Ying, *J. Am. Chem. Soc.* **2008**, *130*, 12586–12587.
[28] a) D. I. Gittins, F. Caruso, *Angew. Chem. Int. Ed.* **2001**, *40*, 3001–3004; b) V. J. Gandubert, R. B. Lennox, *Langmuir* **2005**, *21*, 6532–6539; c) C. Minelli, C. Hinderling, H. Heinzelmann, R. Pugin, M. Liley, *Langmuir* **2005**, *21*, 7080–7082.
[29] E. M. Barranco, O. Crespo, M. C. Gimeno, P. G. Jones, A. Laguna, *Eur. J. Inorg. Chem.* **2004**, 4820–4827.
[30] a) A. D. Becke, *J. Chem. Phys.* **1993**, *98*, 5648–5652; b) C. Lee, W. Yang, R. G. Parr, *Phys. Rev. B* **1988**, *37*, 785–789; c) P. J. Hay, W. R. Wadt, *J. Chem. Phys.* **1985**, *82*, 299–310.
[31] a) R. E. Stratmann, G. E. Scuseria, M. J. Frisch, *J. Chem. Phys.* **1998**, *109*, 8218–8224; b) R. Bauernschmitt, R. Ahlrichs, *Chem. Phys. Lett.* **1996**, *256*, 454–464; c) M. E. Casida, C. Jamorski, K. C. Casida, D. R. Salahub, *J. Chem. Phys.* **1998**, *108*, 4439–4449.
[32] B. C. Tzeng, J. H. Liao, G. H. Lee, S. M. Peng, *Inorg. Chim. Acta* **2004**, *357*, 1405–1410.
[33] B. Guan, D. Xing, G. Cai, X. Wan, N. Yu, Z. Fang, L. Yang, Z. Shi, *J. Am. Chem. Soc.* **2005**, *127*, 18004–18005.
[34] H. Tsunoyama, H. Sakurai, Y. Negishi, T. Tsukuda, *J. Am. Chem. Soc.* **2005**, *127*, 9374–9375.
[35] G. M. Sheldrick, *SHELXL97*, University of Göttingen, Germany, **1997**.
[36] M. J. Frisch, G. W. Trucks, H. B. Schlegel, G. E. Scuseria, M. A. Robb, J. R. Cheeseman, J. A. Montgomery, Jr., T. Vreven, K. N. Kudin, J. C. Burant, J. M. Millam, S. S. Iyengar, J. Tomasi, V. Barone, B. Mennucci, M. Cossi, G. Scalmani, N. Rega, G. A. Petersson, H. Nakatsuji, M. Hada, M. Ehara, K. Toyota, R. Fukuda, J. Hasegawa, M. Ishida, T. Nakajima, Y. Honda, O. Kitao, H. Nakai, M. Klene, X. Li, J. E. Knox, H. P. Hratchian, J. B. Cross, V. Bakken, C. Adamo, J. Jaramillo, R. Gomperts, R. E. Stratmann, O. Yazyev, A. J. Austin, R. Cammi, C. Pomelli, J. W. Ochterski, P. Y. Ayala, K. Morokuma, G. A. Voth, P. Salvador, J. J. Dannenberg, V. G. Zakrzewski, S. Dapprich, A. D. Daniels, M. C. Strain, O. Farkas, D. K. Malick, A. D. Rabuck, K. Raghavachari, J. B. Foresman, J. V. Ortiz, Q. Cui, A. G. Baboul, S. Clifford, J. Cioslowski, B. B. Stefanov, G. Liu, A. Liashenko, P. Piskorz, I. Komaromi, R. L. Martin, D. J. Fox, T. Keith, M. A. Al-Laham, C. Y. Peng, A. Nanayakkara, M. Challacombe, P. M. W. Gill, B. Johnson, W. Chen, M. W. Wong, C. Gonzalez, J. A. Pople, *GAUSSIAN 03*, revision C.02, Gaussian, Inc., Wallingford, CT, **2004**.

Received: December 7, 2008
Published Online: March 12, 2009

